

# Determination of the Solar Radius based on the Annular Solar Eclipse of 15 January 2010

J. Adassuriya<sup>1</sup>, S. Gunasekera<sup>1</sup>, N. Samarasinha<sup>2</sup>

<sup>1</sup> Arthur C Clarke Institute, Katubedda, Moratuwa, Sri Lanka

<sup>2</sup> Planetary Science Institute, Tucson, AZ, USA

e-mail: adassuriya@accmt.ac.lk

Accepted: 07 October 2011

**Abstract.** A determination of the solar radius was made based on the observations of Baily's beads carried out on the southern limit of the annular solar eclipse on 15 January, 2010 from Sri Lanka. A positive correction of  $\Delta R = 0.26 \pm 0.18$  arcsec was found with respect to the standard solar radius,  $R$ , of 959.63 arcsec. The values of  $\Delta R$  from the past observations were analyzed with the phase of the solar activity and found that the magnitude of  $\Delta R$  is maximum at low active phases while it was minimum at high active phases.

© 2011 BBSCS RN SWS. All rights reserved

**Keywords:** Solar Radius, Positive Correction, Activity Phase

## 1. Introduction

The accurate determination of the solar radius is vital to understand the variations of solar irradiance, to assess the effective temperatures and magnetic fields of the sun, and thereby to investigate the effects on the Earth and the near-Earth environment. Among the several techniques used to estimate the solar radius, the eclipse observations have been the most widely used ground-based approach during the past three decades.

The English astronomer, Francis Baily, first noticed the beads, which now bear his name, during the annular solar eclipse on 15 May, 1836. The surface of the moon is not smooth but full of mountains and valleys. When the moon's limb grazes the solar photosphere during a solar eclipse, the light disappears and reappears according to the lunar terrain at the limb. These "blobs" of light manifesting at the limb of the moon with a bead-like appearance during a solar eclipse, are Baily's beads [10]. The timing of the appearance and disappearance of the Baily's beads can be used to estimate the variation of the solar radius from its standard value with an accuracy up to 0.01 arcsec [3]. The accuracy of the estimates of the solar radius depends on the timing of the beads and the lunar limb profile that causes the beads. The Occult 4 software adopted for our analysis is updated with the currently available most accurate lunar limb profile, the Kaguya Lunar Explorer data.

The annular solar eclipse on 15 January, 2010 of Saros 141 cycle had a duration of 11min 8 sec at its greatest [2]. It is the longest annular eclipse until the annular eclipse of 23 December 3043 [4]. On 15 January, 2010, the greatest eclipse occurred at the middle of the Indian ocean at 07:06:33.1 UT with  $\gamma = 0.4$ , where  $\gamma$  is the distance between the axis of the lunar shadow and the center of the Earth, with a magnitude of 0.919 [2].

## 2. Instruments and Observations

The solar eclipse was observed from Sri Lanka by two teams of the Arthur C Clarke Institute, one located close to the centerline and the other at the southern limit.

### 2.1 Centerline Station

The centerline group was located close to the Jaffna city (400 km from the capital city, Colombo) at geographical coordinates of  $9^{\circ} 39' 43.92''$  N and  $80^{\circ} 0' 47.88''$  E which is 14 km away from the centerline. The team was equipped with a Celestron 2800 mm f/10 Schmidt-Cassegrain telescope with a Nikon Coolpix digital camera, where the images were transmitted to a 32-inch Panasonic LCD Screen.

### 2.2 Southern Limit Station

The southern limit station was close to the town, Chilaw (70 km away from Colombo), at geographical coordinates of  $7^{\circ} 40' 6.81''$  N and  $79^{\circ} 49' 50.06''$  E and an altitude of 4 m. This station was located 1.7 km inside the south limit of the eclipse. The team was equipped with a Vixen 720 mm f/9 refractor and a Mead ETX 1250 mm f/13.8 reflector piggybacked on a 12 inch LX200 Schmidt-Cassegrain

which can track the sun (see fig.1). The Mead ETX was used for a live web cast and the Vixen refractor was coupled with a Sony Handy Cam, which has a data transfer rate of 1/30 sec. The latter was equipped with a Baader AstroSolar filter with neutral density rating of 5. The UTC timings and the location were set by the Furuno GPS module ( $\pm 15$  m horizontal error) and the video camera time was synchronized to GPS at the beginning of the observation and again checked for time differences at the end of the observation. This



Fig. 1. Complete setup of the eclipse observation. 720 mm Vixen refractor and 1250 mm ETX Maksutov Cassegrain reflector were piggybacked on the 12 inch LX200 Mead with the tracking system.

procedure had to be performed because of the unavailability of a GPS time inserter in the video camera.

The eclipse phases relevant for this study were recorded from 7:49:37 UT to 7:51:49 UT providing 3960 video frames. Despite using a heavy-duty tripod, the strong winds at the observation site affected the video frames thus requiring great care in the analysis.

Furuno GPS module. In order to find out the time differences between the video camera and the GPS, the time displayed on the GPS was recorded before and after the beads observation.

With the help of video editing software, Edius-5, the delays and fluctuations of the time on the video frames with reference to the GPS time were determined. The difference of the time between the GPS display on the video and the internal clock of the video camera were plotted for the two recordings taken before and after the beads observations (see figs. 2 and 3 respectively). The minimum delay between the GPS and the Video camera was found to be 0.2 sec prior to the beads observation and 0.6 sec after 2.16 hours of observing the eclipse. Although this synchronization error is unavoidable due to the unavailability of GPS time inserter it was considered carefully and corrected as a systematic error. If we assume that the GPS time was consistent, a 0.4 sec time delay had accumulated in the video camera after 2.16 hours of beads observations.

Therefore, we had to correct the delay in the time of the video camera of each individual frame of our Bailly's beads observation video, which contains 3960 individual video frames. In order to correct this time delay, a linear interpolation was done and 0.25 sec were added to the time of the video frames where beads were emerging and 0.26 sec were added to the time of the video frames where beads were disappearing.

### 3.2 Identification of the frames of appearing and disappearing beads

The Limovie (Ver.0.9.26) ([http://www005.upp.sonet.ne.jp/k\\_miyash/occ02/limovie\\_en.html](http://www005.upp.sonet.ne.jp/k_miyash/occ02/limovie_en.html)) software was used to analyze the video frames one by one to find out the exact appearing/disappearing frame of the beads. There were four appearing and four disappearing beads identified in the video by matching the occurrence of simulated beads in the lunar terrain in Occult 4 software. For a selected bead, frame-by-frame analysis was done for a suitable aperture which included the bead, and measurements of the intensity variation were made as a function of the frame number. The distribution was approximated by fitting a polynomial using the MATLAB curve-fitting tool (fig. 4). Subsequently, the variation of the first derivative (rate of change of intensity per frame) was obtained to see the sudden drops (for disappearing beads) or rises (for appearing beads), which can be considered as the disappearing or appearing frame of the bead (fig. 5). Furthermore the contour plots of the video frames in the vicinity of appearance/disappearance were obtained using MATLAB to ensure robustness of the appearing or disappearing frame determined by the intensity variation method. In the contours, the intensity of the pixels is given in the z-axis with the gray scale of 255 levels in x-y plane and approximately one third of 255 is set as the cutoff to identify the appearing/disappearing frame. The frame determined by this method is consistent with the frame determined by the intensity variation method since the differences always lie within five frames. However this method depends on the intensity variation on the vicinity of bead including few pixels which may easily affect the background intensity variations. The clearness of the background in the

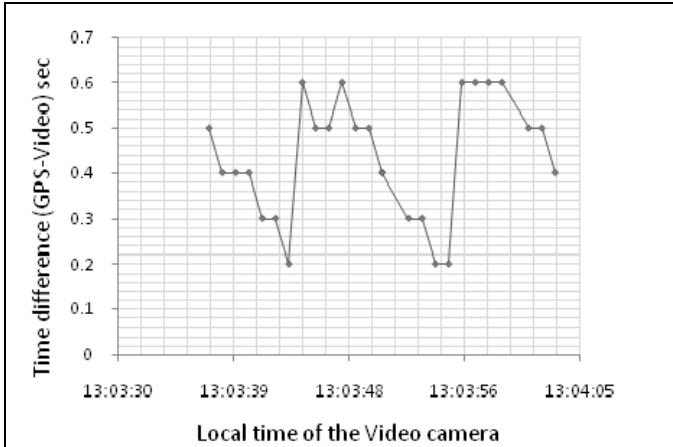


Fig. 2. Delay of the video time with respect to the GPS time for 40 sec before the beads observation of the eclipse.

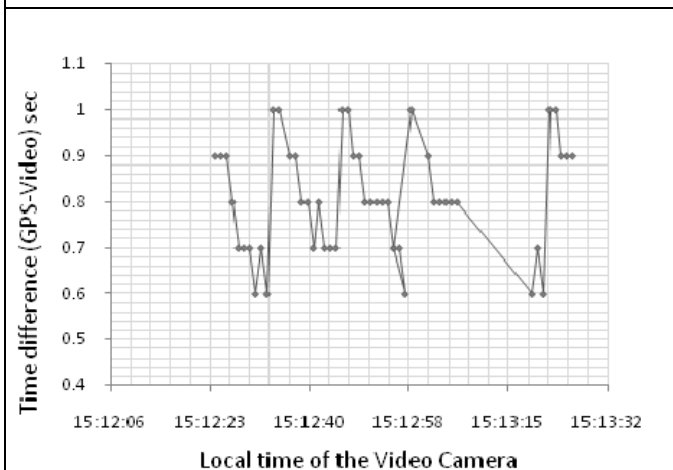


Fig. 3. Delay of the video time with respect to GPS time for 80 seconds after the observation of the eclipse. 2.16 hours had elapsed after the beads observation.

## 3. Data Analysis

### 3.1 Time Correction of Bailly's Beads

Accurate determination of the solar radius highly depends on the identification of the exact timings of the appearing/disappearing of beads. Since our Bailly's beads observation video provides 30 frames per sec, the time of appearing/disappearing of a bead can be determined to 0.03 sec accuracy. As a GPS time inserter was not available to us, the time stamp of the internal clock of the video camera was registered on each video frame of our observation. Before beginning of the solar eclipse, the clock of the video camera was set as accurately as possible with UT time displayed on the

vicinity of the bead is essential to determine the exact frame of appearance/disappearance from this method.

#### 4. Results

The standard angular solar radius at unit distance is 959.63 aresec [7]. All eclipse data refer to this standard value to evaluate any radius changes. Initially the lunar valleys responsible for formation of Bailey's beads were identified using the bead simulation by Occult 4.0.8.6 package running with DE423/LE423 JPL ephemerides. Once the time of appearing or disappearing of a bead on the video is determined, as accurate as possible, using the Limovie software, this time can be input into

the Occult software to find the differences of the moon's limb and the Sun's limb from the mean limb profile of the moon (fig. 6). When the cursor is placed on the valley of the moon's limb which is responsible for the bead in the "Limb Plot" window of the Occult user interface, the differences of the height of the moon's limb and the sun's limb are given on the "limb heights" window with respect to the Watts angle, the angle of the event around the limb of the moon measured eastward from the moon's north pole.

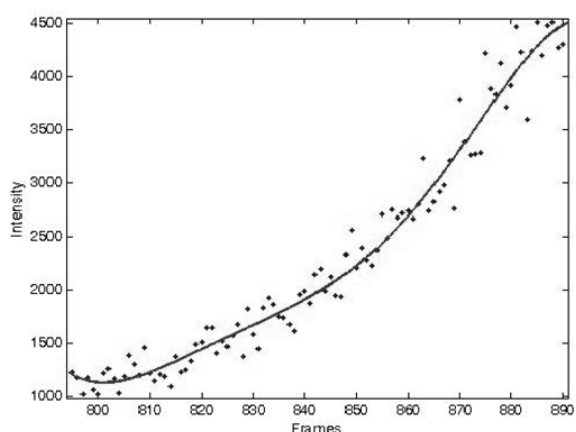


Fig. 4. Intensity of an appearing bead is plotted against the selected frames close to the appearances. A 5<sup>th</sup> degree polynomial is fitted with Root Mean Square Error (RMSE) of 148.4.

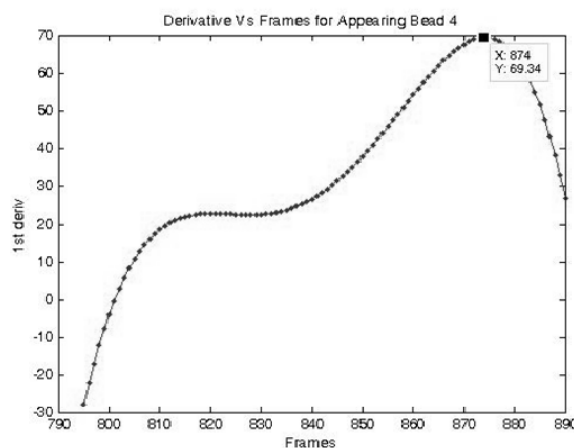


Fig. 5. The first derivative versus frame is obtained to determine the frame of the appearance. The first derivative (The rate of change of intensity) is maximum at frame number 874, which is considered as the frame of appearance.

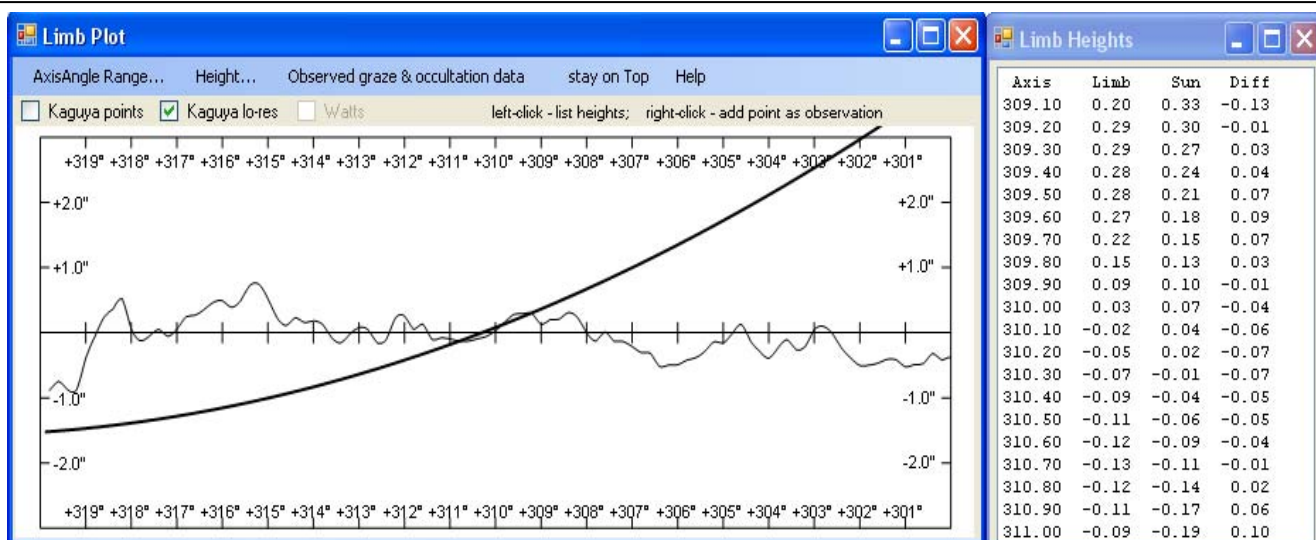


Fig. 6. The Bailey's beads prediction by the Occult (version 4.0.8.6) in the range of 301-319 degrees of the lunar limb and the corresponding limb heights. The thick line indicates the solar limb and the lunar terrain is represented by the thin line. <http://www.lunar-occultations.com/iota/occult4.htm>

**TABLE 1. Bailly's beads events for the annular solar eclipse 15 January 2010. A - appearing beads, D - disappearing beads. The limb heights and Δh were taken from Occult 4.0.8.6 software. WA - Watts' angle**

Bead No	Video Frame No.	WA	Occult Time UT	Observed Time UT	Positive Error with GPS (sec.)	Corrected Time UT (h:m:s)	Moon Limb (")	Solar Limb (")	Δh = (M-S) (")
A <sub>1</sub>	347	310.3	07:49:47.4	07:49:45.87	0.25	07:49:46.12	-0.07	-0.14	0.07
A <sub>2</sub>	484	332.3	07:49:54.4	07:49:50.67	0.25	07:49:50.92	-1.22	-1.41	0.19
A <sub>3</sub>	654	319.0	07:49:57.3	07:49:56.07	0.25	07:49:56.32	-0.37	-0.90	0.53
A <sub>4</sub>	874	317.7	07:50:06.3	07:50:03.07	0.25	07:50:03.32	-0.10	-0.26	0.16
D <sub>1</sub>	3854	338.6	07:51:39.0	07:51:43.17	0.26	07:51:43.43	-0.54	-0.90	0.36
D <sub>2</sub>	3747	342.8	07:51:37.0	07:51:39.47	0.26	07:51:39.73	-0.55	-1.03	0.48
D <sub>3</sub>	3668	346.2	07:51:36.2	07:51:37.00	0.26	07:51:37.26	-0.72	-0.79	0.07
D <sub>4</sub>	3835	347.6	07:51:40.6	07:51:42.53	0.26	07:51:42.79	-0.75	-1.00	0.25

The deviations of the moon's limb and sun's limb from the mean limb of the moon and the corresponding residual (Δh) for eight beads were obtained using Occult and listed in Table 1. Both appearing and disappearing beads show a positive Δh which means the solar radius has to be larger than the standard value (959.63 arcsec). The average of eight beads yields the deviation of the solar radius ΔR= +0.26"± 0.18" where 0.18" is the standard deviation of Δh (or ΔR) values.

**5. Discussion**

From the analysis of the annular solar eclipse of 15 January, 2010, it was determined that the solar radius is 959.89±0.18 arcsec, i.e., with a positive correction of ΔR = 0.26 arcsec, to the standard value 959.63 arcsec. The ΔR was corrected to the distance 1 AU for the observation site located at a distance of 0.9837 AU on 15 January, 2010. The corrected value is 0.25576 arcsec and considered to be 0.26 after round off. This was the first estimation of ΔR in the beginning of the 24th solar cycle, which predicted to have a maximum in 2013 [1]. Due to the limitation of equipments, we were able to handle only one observation site at the south limit. This allowed beads in the range of Watts's angles 310.3° to 347.6° to be monitored. Although it is not statistically sufficient for high accuracy correction, the positive value of the correction provides a good indicator as to how the solar radius varies from its standard value especially during the beginning of the solar cycle 24.

The strong winds at the observation site caused an unsteady imaging system and hence making the analysis inconvenient with Limovie package. Frames were examined with great care to measure the intensity by selecting appropriate aperture sizes for the beads and the backgrounds. To maximize S/N ratio of the intensity of the bead, radius of the aperture bead was selected as approximately one-third of the number of pixels of the background aperture. This allows the background signal to be derived as correctly as possible. The background aperture was either circular or arc appropriately to avoid the interference of the sun light to the background and hence clearly determine the background signal. The approximation of the appearing/disappearing of Bailly's beads is 5 frames from the exact which gives a time uncertainty of 0.17 sec. The error due to the uncertainty, ±0.02 arcsec, is infinitesimal compared the statistical error of eight values.

The sign of the ΔR is stressed rather than the value of it because of the small number of beads observed. Compared to the previous observations by others, a large positive value, ΔR = +0.26 was observed suggesting the effective solar radius was larger than its mean value at the time of the eclipse. The effect of solar active regions near the solar limb had to be considered with great care in this study. However during the period of the eclipse the sun was in its minimum active cycle with a corresponding monthly mean sunspot number of 13.3 for January 2010.

The south limit was pointed at 331o [9] on the solar limb and the beads were occurred 37o around this point. The images taken from SOHO confirmed that there are no active regions of faculae present in the vicinity of this study. The image taken by Locarno Sunspot Drawing [13], Switzerland on 15 January 2010 at 8.30 UT was the closest observation to our study. The detail study of this image shows there is one group of sunspots at +24o from the solar equator and 40o westward from the solar center. The observation of the Bailly's beads were carried out around +60o from the solar equator and at the western solar limb which means 90o from the visible solar center. Therefore the effect of the only sunspot region is zero.

An additional study was carried out to figure out correlation between the activity cycle of the sun with the ΔR for the observations from 1960 to 2010. In this, the solar activity is represented as a phase by using the monthly averaged sunspot number [12] for the duration from 1960 to 2010. The equations 1 and 2 were used for the phase (f) conversion.

$$f = 0.5 \left[ \frac{S - S_{min}}{S_{max} - S_{min}} \right] \dots\dots (1)$$

$$f = 0.5 + 0.5 \left[ \frac{S_{max} - S}{S_{max} - S_{min}} \right] \dots\dots (2)$$

Where S is the sunspot number at any given time for a given sunspot cycle, Smax is the maximum sunspot number and Smin is the minimum sunspot number for that cycle. The equation (1) represents the rising phase of the solar cycle which denotes the range from 0.0 to 0.5 and the equation (2) represents the falling phase which ranges from 0.5 to 1.0. In this way the activity

becomes maximum at the phase of 0.5 and minimum at 0.0 and 1.0 phase. The available  $\Delta R$  values are within the 20th, 21st, 22nd, 23rd and early 24th solar cycles. Those were converted to the phases using the above equations. For the 24th solar cycle,  $S_{max}$  was taken as 90 [1] based on the prediction by Internal Space Environment Service (ISES).

The distribution of  $\Delta R$  versus  $f$  shown in fig. 7 indicates that the magnitude of  $\Delta R$ , increases considerably at low active phases near 0.0 and 1.0 while it tends to a minimum at higher active phase near 0.5. Two quadratic polynomials, fitted separately for positive and negative  $\Delta R$  to approximate the correlation of  $\Delta R$  versus  $f$ , reinforce the tendency of  $\Delta R$  to vary significantly at low active phase of the sun. However the R-square, the square of the correlation between the response values and the predicted response values of the two fits were around 0.2, meaning that the fits cannot be used for precise numerical predictions. The convergence of the  $\Delta R$  with the increase of sunspots was also observed by C. Sigismondi, A. Kilciki [7]. In their studies the  $\Delta R$  values were plotted against the sunspot number in the corresponding period which may hardly detect any sequence. We approach a different attempt and calculate the phase of the solar activity using 4 solar cycles, which gives a better overall view of the  $\Delta R$  and solar activity. In the study of solar radius measurements by Mount Wilson Observatory from 1975 to 2004 [8], if a standard value was assigned around 959.5 arcsec, similar but a weak correlation was noted. However the results from the space-based measurements, done by Kuhn J.K., Emilio M. [6], were quite different as there is no significant changes in solar radius that is synchronous with the solar cycle. This latter study was carried out using SOHO, MDI data within the period from 1996 to 2010, which was in the 23rd solar cycle. Although the ground-based measurements used in our paper are not as frequent as the space-based measurements, they were taken in five different solar cycles with considerable time gaps, which allows on to correlate  $\Delta R$  with solar activity.

Another attempt was made to interpret the variation of  $\Delta R$  within a solar cycle and at the transitions from one cycle to another with respect to the standard value (Fig. 8). The  $\Delta R$  varies by relatively large amounts in the 20th, 21st and 23rd cycles while for the 22nd cycle; the overall radius change is almost constant within the cycle. Within a solar cycle, the fluctuation of  $\Delta R$  from the standard value has means the sun seems to be oscillating through the standard radius but could not fit with the existing 22-year magnetic cycle or the variation of solar irradiance within the period of 1960-2010. Further observations of  $\Delta R$  are needed to clarify the uncertainties present and to quantify the changes over many solar cycles.

The intrinsic change in the solar radius measured by Kuhn J.K., Emilio M. [6] using SOHO data was in milli-arcsec (mas) range and suggests the changes of the order of 0.1 arcsec based on ground-based eclipse observations are unlikely. According to them the ground-based observations are limited by atmospheric seeing thereby resulting in larger  $\Delta R$  [5].

The Bailey's bead observations were carried out only in the vicinity of north and south limit of the eclipse. For

the five eclipses from 2006 (Fig. 9) the average deviation of the north or south limit is 61o from the sun's equator so that the equator zone was hardly encountered; therefore the analysis of  $\Delta R$  from this method is fairer for the Polar Regions. Although this limitation occurs it would be an advantage in this method since the active regions of the sun are located within 30o from the solar equator even in the minimum phase. Therefore, the influence of the active regions to the determination of  $\Delta R$  is minimal. In general the influence of presence of structures on the solar limb is well established, but the possibility to have structures under all beads is statistically low, and even if it is present under one valley, its contribution is divided by number of beads to the final average.

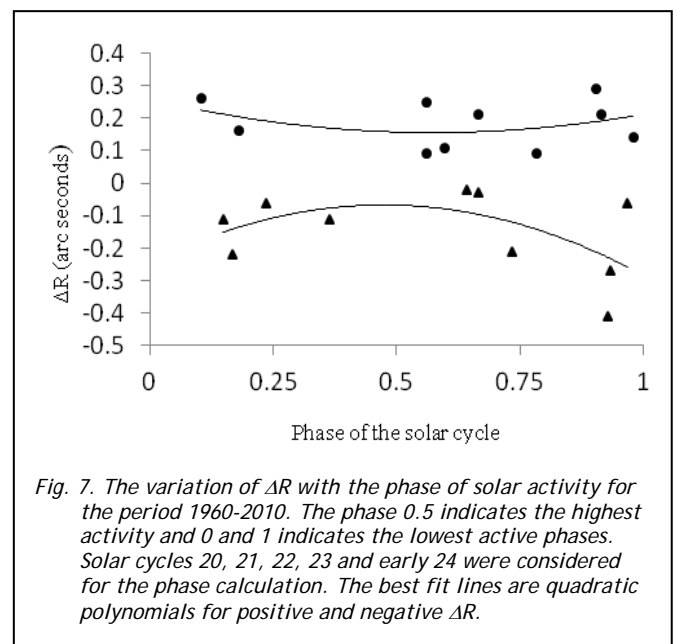


Fig. 7. The variation of  $\Delta R$  with the phase of solar activity for the period 1960-2010. The phase 0.5 indicates the highest activity and 0 and 1 indicates the lowest active phases. Solar cycles 20, 21, 22, 23 and early 24 were considered for the phase calculation. The best fit lines are quadratic polynomials for positive and negative  $\Delta R$ .

## 6. Conclusions

The solar radius was calculated by means of the annular solar eclipse as observed from Sri Lanka on 15 January 2010, and found to be  $959.89 \pm 0.18$  arcsec. This is the first estimate during the beginning phase of the 24th solar cycle. The magnitude of  $\Delta R$  is minimum at the high active phases of the solar cycle and maximum at the low active phases. There is no clear correlation with the sign of  $\Delta R$  and the solar cycle. Within a solar cycle, the variation of solar radius is not completely random but likely to increase or decrease through the standard radius. No definite pattern for the behavior of  $\Delta R$  from one cycle to another was found.

## Acknowledgements

Special thank goes to Mr. Jayathu Fernando of Arthur C Clarke Institute for providing the Sony Handy Cam for the observations and Mr. Indika Madagangoda, also of the same institute, for coordinating the observations at the centerline of the eclipse. The authors wish to thank Dr. C. Sigismondi for his valuable comments throughout the project and Dr. Sushant Tripathy for pointing out the space-based observations. The sunspot data are taken from Solar Influence Data Analysis Center, Royal Observatory of Belgium.

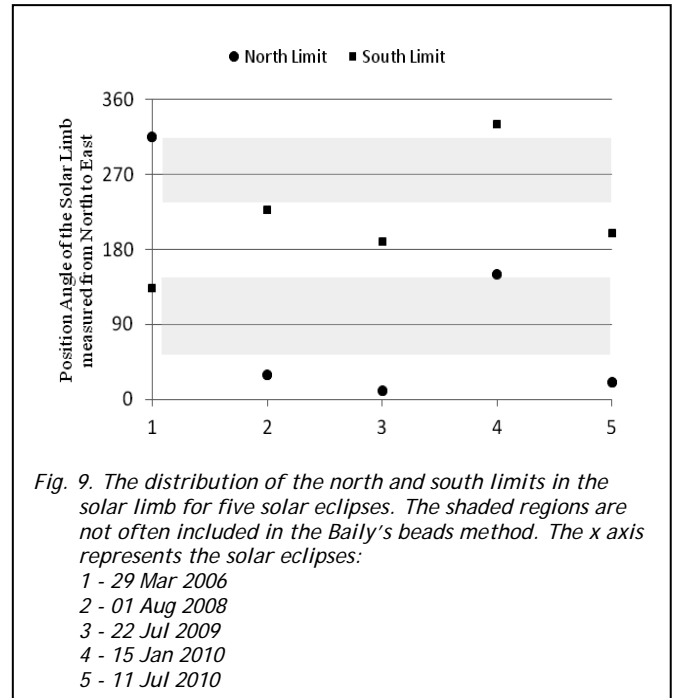
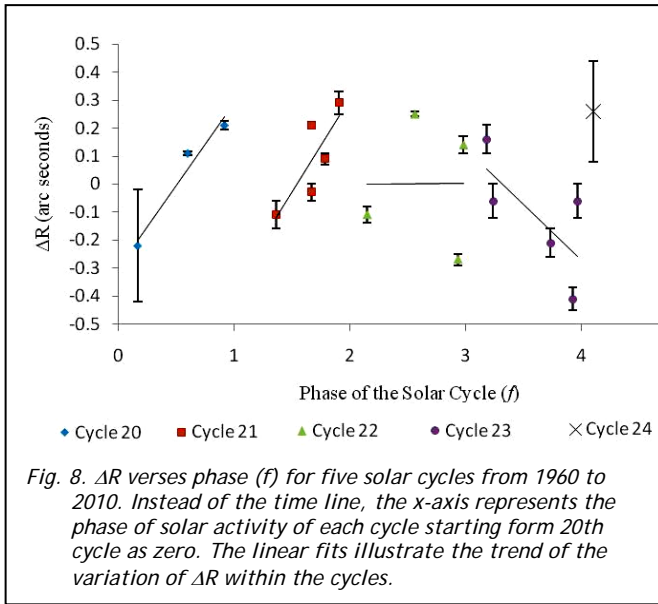


**TABLE 2. Previous observations of  $\Delta R$  with respect to the standard value of 959.63" from 1715 to 2010. This is adopted from A. Kilcik, C. Sigismondi et al. 2009. The last observation, 15th January 2010 is from our results.**

Date	Eclipse type	Number of obs.	$\Delta R$ ["]
1715 May 3	Total	3	+0.48 ± 0.20
1925 Jan 24	Total	8	+0.51 ± 0.08
1966 May 20	Hybrid	20	- 0.22 ± 0.20
1970 Mar 7	Total	300	+0.11 ± 0.008
1973 June 30	Total	85	+0.21 ± 0.015
1976 Oct 25	Total	43	+0.04 ± 0.07
1979 Feb 26	Total	47	- 0.11 ± 0.05
1980 Feb 16	Total	232	- 0.03 ± 0.03
1980 Feb 16	Total	135	+ 0.21 ± 0.0012
1981 Feb 4	Annular	153	- 0.02 ± 0.03
1983 June 11	Total	201	+0.09 ± 0.02
1984 May 30	Hybrid	51	+0.29 ± 0.04
1984 May 30	Hybrid	51	+0.09 ± 0.04
1987 Sep 23	Annular	123	- 0.11 ± 0.03
1991 July 11	Total	59	+0.09 ± 0.10
1991 July 11	Total	300	+0.25 ± 0.008
1994 May 10	Annular	53	- 0.27 ± 0.02
1995 Oct 24	Total	92	+0.14 ± 0.03
1998 Feb 26	Total	76	+0.16 ± 0.05
1999 Aug 11	Total	58	- 0.06 ± 0.06
2002 Dec 04	Total	58	- 0.21 ± 0.05
2006 Mar 29	Total	35	- 0.41 ± 0.04
2006 Sep 22	Annular	13	-0.06 ± 0.06
2010 Jan 15	Annular	8	+0.26 ± 0.18

**REFERENCES**

- [1] Biesecker, D.: 2008, NOAA, SEC, The Solar Cycle 24 Consensus Prediction.
- [2] Espenak, F. and Anderson, J.: 2008, NASA 2010 Eclipse Bulletin, 1, 40.
- [3] Guilmier, P. and Koutchmy, S.: 1998, Total Eclipses, Springer, p. 58, 82.
- [4] Harrington, P. S.: 1997, Eclipse, John Wiley & Sons, p. 121, 214.
- [5] Kuhn, J. R., Emilio, M. et al.: 2000, The Astrophysical Journal, 1007, 1010.
- [6] Kuhn, J. R., Emilio, M. et al.: 2010, The Astrophysical Journal, 1381, 1385.
- [7] Kilcik, A., Sigismondi, C., Rozelot, J. P, Guhl, K.: 2009, Solar Physics, 237, 250.
- [8] Lefebvre, S., Bertello, L. et al.: 2006, The Astrophysical Journal, 444, 451.
- [9] Lunar Limb Profile: 2010, Annular and Total Solar Eclipses of 2010, NASA
- [10] Nugent, R.: 2007, The IOTA Occultation Observers Manual, 238, 247.
- [11] Sigismondi, C.: 2008, Sci China Ser G-Phys Mech Astron, 1, 7.
- [12] SIDC-team, The International Sunspot Number, Royal Observatory of Belgium, Ringlaan 3, 1180 Brussel, Belgium, 1960 - 2010.
- [13] [Specola Solare Ticinese, Sunspot Data, Locarno